Published in final edited form as:
Sci Transl Med. 2012 February 1; 4(119): 119ra14. doi:10.1126/scitranslmed.3003197.

CXCL12-Induced Monocyte-Endothelial Interactions Promote Lymphocyte Transmigration Across an in Vitro Blood-Brain Barrier

Shumei Man[1], **Barbara Tucky**[1], **Anne Cotleur**[1], **Judith Drazba**[2], **Yukio Takeshita**[1], and **Richard M. Ransohoff**[1,*]

[1]Neuroinflammation Research Center, Department of Neuroscience, Lerner Research Institute, Cleveland Clinic, Cleveland, OH 44195, USA

[2]Imaging Core, Lerner Research Institute, Cleveland Clinic, Cleveland, OH 44195, USA

Abstract

The accumulation of inflammatory cells in the brain parenchyma is a critical step in the pathogenesis of neuroinflammatory diseases such as multiple sclerosis (MS). Chemokines and adhesion molecules orchestrate leukocyte transmigration across the blood-brain barrier (BBB), but the dynamics of chemokine receptor expression during leukocyte transmigration are unclear. We describe an in vitro BBB model system using human brain microvascular endothelial cells that incorporates shear forces mimicking blood flow to elucidate how chemokine receptor expression is modulated during leukocyte transmigration. In the presence of the chemokine CXCL12, we examined modulation of its receptor CXCR4 on human T cells, B cells, and monocytes transmigrating across the BBB under flow conditions. CXCL12 stimulated transmigration of $CD4^+$ and $CD8^+$ T cells, $CD19^+$ B cells, and $CD14^+$ monocytes. Transmigration was blocked by CXCR4-neutralizing antibodies. Unexpectedly, CXCL12 selectively down-regulated CXCR4 on transmigrating monocytes, but not T cells. Monocytes underwent preferential CXCL12-mediated adhesion to the BBB in vitro compared with lymphocytes. These findings provide new insights into leukocyte-endothelial interactions at the BBB under conditions mimicking blood flow and suggest that in vitro BBB models may be useful for identifying chemokine receptors that could be modulated therapeutically to reduce neuroinflammation in diseases such as MS.

INTRODUCTION

Multiple sclerosis (MS) is an inflammatory demyelinating disease of the human central nervous system (CNS). Inflammation initiates the lesions of MS and involves accumulation of blood-derived inflammatory cells in the CNS parenchyma. The inflammatory molecular

*To whom correspondence should be addressed. ransohr@ccf.org.

SUPPLEMENTARY MATERIAL
www.sciencetranslationalmedicine.org/cgi/content/full/4/119/119ra14/DC1
Movie S1. Leukocyte-endothelial interactions movie showing monocytes undergoing preferential CXCL12-dependent adhesion in vitro compared with lymphocytes under flow.

Author contributions: S.M. designed and performed the experiments, analyzed all the data, and wrote the manuscript. B.T. carried out cell culture, PBMC isolation, flow cytometry staining, and image analysis. A.C. operated the LSR II flow cytometry system and participated in lymphocyte isolation and data analysis. J.D. contributed to setting up the TIRF MC System. Y.T. participated in CXCR4 modulation experiments. R.M.R. designed all the experiments, analyzed the data, and wrote the manuscript. All authors participated in the design and interpretation of the experiments and results. All authors contributed toward writing and editing the manuscript.

Competing interests: The authors declare that they have no competing interests.

cascade that leads to CNS tissue infiltration by blood-derived leuko-cytes has been progressively elucidated. This research has led to the hypothesis that leukocytes often initially transmigrate through the blood-brain barrier (BBB) via pial vessels (1, 2) located at the surface of the brain and spinal cord. Pial vessels exhibit interendothelial tight junctions that are characteristic of the BBB. However, being outside the brain parenchyma, pial vessels are not associated with astrocyte end-feet (3). Other sites where leukocytes enter the CNS include the choroid plexus and the BBB within the brain parenchyma (4).

Chemokines and adhesion molecules orchestrate leukocyte trans-endothelial migration (TEM) across the BBB (5–7) and are attractive targets for the development of drugs to manage MS (8, 9). Blockade of leukocyte trafficking into the CNS has been shown to be therapeutically effective, confirming the role of blood-derived leukocytes in MS pathogenesis (10). However, available therapies that inhibit leukocyte trafficking by blocking adhesion molecules carry substantial risks (10), probably related to their action against a wide spectrum of leukocyte populations. More selective means to abrogate leukocyte entry into the CNS of patients with neuroinflammatory diseases such as MS are needed (11). To achieve this goal, we need clearer insights into the mechanisms by which blood-derived leukocytes enter the CNS in health and disease.

Immunohistochemical staining of MS lesions for chemokines and chemokine receptors is an attractive way to initiate studies of leukocyte infiltration of the CNS. However, the complexity of leukocyte transmigration and chemokine receptor modulation challenges the use of immunohistochemical data as a stand-alone means for identifying the best targets for inhibition. This complexity is evident at multiple levels: Chemokine receptors expressed by leukocytes recognize ligand on both the luminal and the abluminal surface of endothelial cells during transmigration into tissue from the flowing blood (12). After ligand exposure, chemokine receptors can be down-regulated and degraded or recycled at different rates (13, 14), resulting in either the absence or the presence of the receptor on migrating cells. Chemokine receptors on defined cell populations (such as naïve monocytes or memory T cells) differ markedly when circulating cells are compared with tissue-infiltrating cells, suggesting dynamic regulation. For example, very few CCR2-positive mononuclear inflammatory cells have been identified in MS lesions by immunohistochemistry compared to >95% of monocytes expressing variable levels of CCR2 in peripheral blood (15). CCL2 immunoreactivity is abundant in active and chronic MS lesions despite decreased CCL2 in the cerebrospinal fluid (CSF) of MS patients, suggesting that ligand (CCL2) might be consumed as its receptor (CCR2) is down-regulated (16). $CCR5^+$ monocytes arrayed in the perivascular spaces around microvessels in MS tissue (an inflammatory finding termed “perivascular cuffing”) comprise more than 50% of infiltrating myeloid cells, although less than 15% of blood monocytes express CCR5 (8, 17). Among CXC chemokines, CXCL12 ligand is particularly associated with leukocyte infiltration of the CNS, and regulation of its receptor CXCR4 is complex. CXCL12 is expressed in several cellular contexts in the CNS (18–20). Neuropathological studies have demonstrated that CXCL12 immunoreactivity is associated with endothelial cells within microvessels in control autopsy human brain sections and exhibits basolateral (abluminal) localization (20), where it serves to restrict the transit of infiltrating leukocytes from perivascular cuffs into the parenchyma (20–22). During CNS inflammation, this polarized expression is altered with loss of perivascular CXCL12 protein and relocation of this chemokine to the luminal side of the vasculature (20–22). CXCR4 and CXCR7, the two receptors that bind to CXCL12, play complementary roles in its function. These receptors belong to a subfamily of heterotrimeric guanine nucleotide–binding protein (G protein)–coupled receptors (GPCRs): CXCR4 ligation triggers $G\alpha_i$ signaling, whereas CXCR7 is not G protein–linked in most cells (23–26) and often serves to localize CXCL12 in tissues by internalization or translocation.

Studies using knockout mice or small-molecule inhibitors (21, 22) indicate that chemokines and their receptors are crucial for selective infiltration of the CNS by subpopulations of leukocytes (27–30). Analyses of chemokines and chemokine receptors in MS lesions, when complemented by mechanistic in vitro transmigration studies to define how individual receptors are regulated on relevant cells, are the best approach for guiding therapeutic development.

Experiments using a static BBB model (without shear forces) have provided provisional answers to questions regarding chemokine receptor modulation and function during leukocyte transmigration (9, 31–33). However, an in vitro model using human umbilical vein endothelial cells (HUVECs) for examining leukocyte-endothelial interactions under physiological shear forces showed convincingly that shear forces promote rather than disrupt the processes required for transmigration, including adhesion, locomotion, and pseudopod formation during the cell's exit from the blood vessel, termed extravasation (12, 34–36). Accordingly, it has become clear that physiologically relevant BBB transmigration assays require incorporation of shear forces.

Here, we report that a new in vitro BBB model under shear forces mimicking blood flow can help to bridge the gap between descriptive immunohistochemical studies and the identification of chemokines and their receptors that could be targeted therapeutically for treating neuroinflammatory diseases. Transfected human brain microvascular endothelial cells (THBMECs) are stable in culture and have BBB features including intercellular tight junction–associated protein expression, modestly elevated transendothelial electrical resistance (compared with HUVECs), and efficient solute exclusion (15, 37, 38). Under physiological flow rates and cytokine cocktail treatments, THBMECs maintain their BBB characteristics (6). Using THBMECs in a modified chemotaxis chamber incorporating shear forces, we assayed how the CXCL12 chemokine andits CXCR4 receptor govern leukocyte transmigration under flow conditions, and also defined how CXCR4 expression on leukocytes is modulated during chemokine binding and leukocyte transmigration across the BBB.

RESULTS

In vitro BBB transmigration assay under flow

The chemotaxis chamber (see Fig. 1) was modified from a Neuro Probe AA12 chemotaxis chamber to enable assays to be conducted under physiological shear forces (flow). The chamber comprises a precision-machined acrylic top, middle, and bottom plates, assembly hardware, a silicone top gasket with a flow area of 16 mm wide, 75 mm long, and 0.8 mm thick, and a silicone bottom gasket (Fig. 1). The plates have 12 wells in two offset rows. Each well in the middle plate is 6.5 mm in diameter and holds 220 μl. Framed polycarbonate membrane filters were manufactured by Neuro Probe to our specifications with a pore size of 3 μm. THBMECs were cultured on rat-tail collagen-coated framed filters to subconfluence and were activated with tumor necrosis factor–α (TNF-α) (10 U/ml) and interferon-γ (IFN-γ) (20 U/ml) for 24 hours at 37°C. The cells were then termed activated THBMECs (aTHBMECs). Transendothelial migration (TEM) buffer containing CXCL12 (25 ng/ml) was incubated with aTHBMECs for 10 min at 37°C. Excess CXCL12 was removed by two washes, and CXCL12 associated with the human endothelial cells was termed apical CXCL12. Another chemokine, CCL2, is abundant in MS lesions (16). To simulate inflammatory conditions and create a chemotactic environment, we loaded CCL2 (25 ng/ml) in TEM buffer in the lower chamber on the abluminal side of the THBMECs (termed basolateral CCL2). Basolateral CCL2 was used in all of the transmigration studies including basal migration where CXCL12 was omitted, with the exception of pertussis toxin (PTX) pretreatment experiments where basolateral CCL2 was not used to study direct

activation of CXCR4 by CXCL12. The membrane with a confluent layer of aTHBMECs was washed twice with TEM buffer and placed between the top and the bottom plates, and the top gasket was positioned over the filter to create a flow area of about 420 μl. Narrow raised rims of bottom wells mating the membrane frame enhanced the seal. With the apparatus in a 37°C incubator, human peripheral blood mononuclear cells (PBMCs) were perfused across the THBMECs by a Medfusion 3010a pump through the inlet on the top plate. The wall shear stress (τ_w) is related to the volumetric flow rate (Q) by $\tau_w = 6\mu Q/wh^2$, where μ is the fluid viscosity, h is height, and w is width of the flow field (39). The flow rate was 1 ml/s (46 ml/hour), simulating the estimated flow rate in human cerebral capillaries (40). The final shear stress was 0.2 dyne/cm^2. At the end of a defined period of flow, the chamber was disassembled and the framed filter was carefully removed. The cells that had transmigrated across the THBMEC layer were collected from the lower chamber. Flow-through nonmigrating cells were collected from the outlet tubing. Cells that were introduced into the system (termed input cells), migrating cells, and flow-through cells were harvested for quantification and flow cytometry analysis. Chamber calibration was performed every 6 months. Gaskets were replaced regularly to minimize systematic error.

Apical CXCL12 induces transmigration

Using flow cytometry, we found that CXCR4 was expressed by more than 50% of CD4$^+$ T cells, CD8$^+$ T cells, CD14$^+$ B cells, and CD19$^+$ monocytes in the peripheral blood of healthy people (Fig. 2A). It has been reported that CXCR7 is not expressed on human or mouse leukocytes, except for a small subset of B cells (41). Addition of CXCL12 to the top chamber on the apical side of the aTHBMEC layer enhanced PBMC migration compared to aTHBMECs without CXCL12 even though we included CCL2 basolaterally (Fig. 2B). Incubating PBMCs with the anti-CXCR4 antibody 12G5 before the transmigration assay abrogated CXCL12-induced transmigration of immune cells across the aTHBMEC layer (Fig. 2C). In contrast, CXCL12-induced migration was not affected by preincubating PBMCs with the anti-CXCR7 antibody 11G8 (Fig. 2D). It is well established that PTX inhibits $G\alpha_i$ signaling by adenosine diphosphate (ADP) ribosylation. CXCL12-induced migration of PBMCs was inhibited by preincubating PBMCs with PTX (Fig. 2E), indicating that apical CXCL12 stimulated PBMC migration by activating $G\alpha_i$ signaling via CXCR4 receptors.

Apical CXCL12 down-regulates CXCR4 on transmigrating monocytes

To study the modulation of CXCR4 during CXCL12-induced transmigration of PBMCs, we measured CXCR4 fluorescence intensity by flow cytometry on both the input population of PBMCs and the PBMCs that transmigrated across the THBMEC layer. Apical CXCL12 selectively reduced CXCR4 median fluorescence intensity (MFI) of transmigrating monocytes compared to the input population, whereas CXCR4 expressed by CD4$^+$ T cells, CD8$^+$ T cells, and CD19$^+$ B cells was not down-regulated (Fig. 3A). The reduction in CXCR4 MFI on a logarithmic scale was demonstrated in single-channel histograms from flow cytometry analyses, which showed a substantial left shift in CD14$^+$ monocyte CXCR4 intensity during apical CXCL12-induced migration, which was not observed for T or B cells (Fig. 3B). In contrast, when PBMCs were incubated in solution with CXCL12, CXCR4 MFI was reduced on all PBMC subtypes (Fig. 3, C and D), confirming that CXCR4 was capable of being down-modulated by stimulation with the CXCL12 ligand on all PBMC subpopulations. CXCR4 was down-regulated on transmigrating CD14$^+$/CD16$^-$ monocytes (Fig. 3E) compared to CD16$^+$/CD14$^-$ natural killer (NK) cells (Fig. 3F). To confirm that CXCL12 was associated with the THBMEC surface, we performed live-cell staining. Apical CXCL12 formed larger and more numerous apparent aggregates on aTHBMECs (Fig. 4, B and D) compared to the staining on aTHBMECs without exogenous CXCL12 (Fig. 4, A and C). These studies were not performed under flow conditions, because cells were cultured

and imaged on coverslips. Tissue staining of luminal CXCL12 in tissue sections also shows punctate staining consistent with aggregation (20). In summary, the presence of apical CXCL12 in the top chamber induced PBMC transmigration across the aTHBMEC layer and selectively down-regulated CXCR4 expression on monocytes.

CXCL12-induced monocyte-endothelial interactions facilitate lymphocyte transmigration

The fact that apical CXCL12 enhanced migration in all PBMC groups but down-regulated CXCR4 only on monocytes suggested that monocytes selectively respond to apical CXCL12 and that monocyte interactions with endothelium may have then facilitated T and B cell transmigration. To address this possibility, we used negative selection to isolate and assay PBMC subpopulations in our transmigration assay. The purity of isolated lymphocytes (Fig. 5A) and monocytes (Fig. 5B) was confirmed by flow cytometry. Isolated lymphocytes failed to transmigrate in response to CXCL12, whereas the addition of monocytes (at a lymphocyte/monocyte ratio of 4:1, which is found in PBMCs) restored lymphocyte transmigration (Fig. 5C).

These data suggested that CXCL12-dependent monocyte-endothelial cell interactions facilitated T and B cell transmigration across the aTHBMEC layer. Under flow conditions and in response to CXCL12, monocytes in PBMCs seemed to interact more efficiently with endothelium than did PBMC lymphocytes. This possibility was addressed by parallel plate adhesion assays in which lymphocytes and monocytes were individually isolated by negative selection, differentially labeled with CellTracker dyes, and mixed at a ratio of 4:1 (the ratio normally found in PBMCs). Images at the beginning (Fig. 5D) and at the end (Fig. 5E) of the 20-min assay showed that monocytes (yellow) disproportionately adhered to aTHBMECs compared with lymphocytes (magenta). Individual cell motion was further analyzed from a video recording of the adhesion assay (movie S1). Analysis of four experiments showed that monocytes adhered about four times more frequently than did lymphocytes in a 20-min adhesion assay (17 versus 4, $P = 0.02$) despite their lower numbers in the input cell inoculum (Fig. 5F). These observations also excluded the possibility that CCL2 (present in transmigration assays but not in the adhesion assays) was required for the preferential response of monocytes to CXCL12 under flow. The focal plane for these videos was set at the endothelial surface and also demonstrated more nonadherent, reversible monocyte-endothelial interactions.

DISCUSSION

Here, we developed an in vitro model system that allowed us to investigate leukocyte transmigration across BBB endothelium under flow conditions and to analyze chemokine receptor expression by the original input PBMC population, transmigrating PBMCs, and flow-through (nontransmigrating) leukocytes. Next, we showed that the chemokine CXCL12 stimulated lymphocyte and monocyte transmigration across the BBB endothelium. However, CXCL12 induced selective down-regulation of CXCR4 expression by monocytes but not by T and B lymphocytes, which nonetheless expressed functional CXCR4. Then, we found that monocytes selectively adhered to the BBB endothelium under flow in response to CXCL12 and we propose that monocyte-endothelial cell interactions facilitated lymphocyte migration across the BBB endothelium.

In vitro BBB models have provided useful information regarding therapeutic targeting of chemokines and chemokine receptors in the CNS, drug pharmacokinetics, as well as insights into the pathogenesis of neuroinflammation, neurodegeneration, and CNS tumors (42). Models incorporating flow were created to replicate more closely the physiological in vivo environment of the BBB (43) and to integrate shear forces into the analysis of leukocyte-endothelial interactions. Here, we describe an in vitro BBB model that incorporates flow and

enables analysis of chemokine receptor modulation on transmigrating leukocytes. Compared with existing dynamic models (6, 44, 45), an advantage of our model is the opportunity to collect transmigrated cells for phenotyping including chemokine receptor expression.

The chemokine CXCL12 was selected for study because it appears to contribute critically to leukocyte migration across the BBB and from perivascular spaces into CNS parenchyma (20, 22, 46, 47). The complex molecular mechanisms underlying CXCL12 tissue distribution during neuroinflammation are incompletely understood. Chemokines on endothelial luminal surfaces stimulate leukocyte integrin activation, adhesion, and transmigration of leukocytes across the endothelial layer (48–51), whereas chemokines on the abluminal side of the endothelial layer may organize and maintain perivascular leukocyte aggregates (20, 22, 52). Endothelial cell surface glycosaminoglycans immobilize chemokines, typically in oligomers, and enhance their local availability to rolling and crawling leukocytes (53–55). Our live-cell imaging showed apparent CXCL12 aggregates on apical aspects of the cytokine-activated THBMEC layer in vitro that mimics the BBB. CXCL12 distribution is also affected by CXCR7, a nontraditional receptor specific for CXCL11 and CXCL12 that lacks G protein–coupled signaling but internalizes CXCL12 for either lysosomal degradation or transcytosis and redistribution (56, 57). CXCR7 was not present on monocytes or T cells, and CXCR7-mediated transcytosis was not relevant for our model because CXCL12 was available on the apical surface of the THBMECs, corresponding to the vascular lumen.

Chemokine receptors are appealing drug targets for treating neuroinflammatory disease, but the multiplicity of receptors and receptor modulation during ligand-induced transmigration of leukocytes into the CNS complicates identification of appropriate target receptors. Unexpectedly, we found that CXCR4 was selectively down-regulated on monocytes but not lymphocytes during CXCL12-stimulated transmigration of PBMCs across the BBB in our in vitro model system, implying that monocytes selectively use CXCL12/CXCR4 to generate integrin-dependent interactions with BBB endothelium under flow. There are ample precedents for selective cell-specific responses to CXCL12 via CXCR4. For example, signaling to CXCR4 modulates adult hippocampal neural stem cell proliferation, which is primarily governed by γ-aminobutyric acid (GABA) receptor stimulation (58). In contrast, cerebellar granule cell progenitors migrate along a band of CXCL12 at the pial surface and subsequently proliferate through a synergistic response to CXCL12 and sonic hedgehog (59). Quite differently, CXCR4 signaling activated by CXCL12 governs B lymphocyte retention in bone marrow during development (60). Illustrating selective signaling by chemokines to receptor-bearing cells, we previously reported that CX3CR1 is broadly expressed on blood lymphocytes and monocytes but only signals to NK cells for recruitment to the CNS in the experimental autoimmune encephalomyelitis (EAE) mouse model of MS, despite free CX3CL1 ligand that was available for signaling to other receptor-bearing cells (30). In separate studies of PBMC migration in vitro under flow, we found that abluminal CCL2 induced lymphocyte and monocyte migration but selectively down-regulated monocyte CCR2. This finding was in agreement with our previous report that infiltrating monocytes in MS lesions lack surface CCR2 (15).

Here, we report that a single cell type in PBMCs responds selectively to a native chemokine based on its presentation on the apical surface of the THBMEC layer, rather than in solution. This selective response might be dictated in part by the physical state of the immobilized chemokine. A mutant obligate monomer CCL2 peptide that is unable to oligomerize could readily induce chemotaxis of monocytes in a Transwell chamber assay, but was not able to attract monocytes into the inflamed CNS in EAE mice (61). Mutant CCL5, which was not able to bind to glycosaminoglycans, also activated signaling in solution but was unable to mediate leukocyte recruitment in vivo (61). Our live-cell imaging analyses suggested that

CXCL12 formed aggregates on the apical surface of aTHBMECs. We speculate that CXCL12-mediated differential signaling to monocytes but not lymphocytes under flow was contingent on the "presentation" of CXCL12 on the apical surface of aTHBMECs, possibly in the form of oligomeric aggregates. Notably, structural modeling has demonstrated how chemokine polymers could be assembled on tissue surfaces (62).

Monocyte removal from PBMCs abrogated lymphocyte transmigration under flow, an effect that was reversed by adding back the monocytes. These data suggested that monocytes were induced by CXCL12 to promote lymphocyte transmigration. All PBMC subtypes failed to transmigrate under basal conditions in the absence of CXCL12. Several possibilities exist to account for these observations: First, adherent monocytes might interact physically with lymphocytes, "trapping" them before transmigration. Our imaging studies argue against this possibility because monocytes and lymphocytes did not form evident physical contacts (movie S1). Second, monocytes could potentially elaborate cytokines or proteolytic enzymes such as matrix metalloproteinases or cathepsins that might expose ligands mediating adhesion and thereby modify THBMECs to become more permissive for interaction with lymphocytes. CXCL12 might trigger monocytes to secrete chemokines that directly induce lymphocyte adhesion to THBMECs. Physical interaction between adherent monocytes and endothelial cell apical surfaces might induce THBMEC alterations that enhance lymphocyte adhesion. We note that these possibilities are not mutually exclusive given the array of effector properties expressed by monocytes and the complex, stepwise character of leukocyte-endothelial interactions under flow.

Results presented here should be interpreted with recognition of the limitations of our model system. The experiments were done using a single line of THBMECs, which were transformed with simian virus 40 (SV40) T antigen. Extending the studies using additional HBMECs cell lines as well as primary HBMECs will be useful to define how consistently these observations can be replicated with different sources of HBMECs. Additionally, the present studies were done using HBMECs without coculture, mimicking the BBB of the pial vasculature. Including pericytes and astrocytes, the accessory cells of the parenchymal BBB, will permit a fuller analysis of the interactions of leukocytes with cellular elements of the BBB under flow and, in turn, will sharpen our understanding of appropriate therapeutic targets.

The present results are broadly concordant with a recent report using *Ccl2*$^{-/-}$ mice with coronavirus encephalitis and showing that CNS perivascular monocytes promoted lymphocytes to enter the inflamed parenchyma across the glia limitans, a network of glial cell processes and a basement membrane that together separate the brain parenchyma from the CNS perivascular space (63). The present report extends those findings and provides proof of principle that complementary data from dynamic BBB models in vitro, validated by immunohistochemical analysis of inflamed human CNS tissue and animal model research, will be instrumental for selecting therapeutic targets to modulate leukocyte infiltration of the CNS in neuroinflammatory diseases such as MS.

MATERIALS AND METHODS

Human subjects and reagents

Healthy volunteers between 20 and 50 years old were recruited. All study protocols were approved by the Cleveland Clinic Institutional Review Board, and signed informed consents were obtained from all blood donors. Subjects were not experiencing systemic infection or taking non-steroidal anti-inflammatory drugs (NSAIDs) at the time of phlebotomy. Anti-human antibodies used include mouse anti-CXCR4 monoclonal 12G5 [provided by the National Institutes of Health (NIH) AIDS Research and Reference Reagent Program],

mouse immunoglobulin G2A (IgG2A) (MAB003, R&D Systems), anti-CXCR7 11G8 (ChemoCentryx Inc.), mouse IgG (Invitrogen), anti-CXCR4 allophycocyanin (clone 12G5, BD Biosciences), anti-CD4 phycoerythrin–Alexa Fluor 610 (clone S3.5, Invitrogen), anti-CD8 Pacific Orange (clone 3B5, Invitrogen), anti-CD14 peridinin chlorophyll protein (clone MφP9, BD Biosciences), anti-CD19 Pacific Blue (clone SJ25-C1, Invitrogen), and rabbit anti-CXCL12 (PeproTech). Recombinant human CXCL12 and CCL2 were from R&D Systems. Human CD14 MicroBeads were from Miltenyi Biotec. Human Monocyte Enrichment without CD16 Depletion Kit was from Stemcell Technologies. LinearFlow Flow Cytometry Intensity Calibration kit, CellTracker Green CMFDA, and CellTracker Red CMTPX were from Invitrogen. Parallel Plate Flow Chamber was purchased from GlycoTech.

Cell culture and PBMC isolation

THBMECs are adult human brain endothelial cells transfected and immortalized with plasmid containing SV40 large T antigen as previously described (15, 31, 37). THBMECs were grown in RPMI 1640 containing 10% heat-inactivated fetal bovine serum, 10% Nu-Serum, 2 mM glutamine, 1 mM pyruvate, essential amino acids, and vitamins. PBMCs were isolated from fresh heparinized blood of healthy subjects by density centrifugation with Lymphocyte Separation Medium (Mediatech) as previously described (15, 31, 37). PBMCs were resuspended at 5×10^5 cells/ml in TEM buffer (RPMI 1640 without phenol red + 1% bovine serum albumin + 1 mM Hepes) for transmigration assays and assayed within 2 hours of phlebotomy.

Flow cytometry

PBMCs were blocked with mouse IgG and then stained with fluorescently conjugated antibodies for CXCR4, CD4, CD8, CD14, and CD19. Data were acquired with an LSR II flow cytometer (BD Biosciences). Analysis was carried out with FlowJo version 9 (Tree Star Inc.). Lymphocytes and monocytes were gated according to forward and side scatter, as well as antibody staining profiles. To verify the specificity of the anti-CXCR4 antibody 12G5, we incubated nonconjugated antibody 12G5 (30 μg/ml) with PBMCs for 15 min at 4°C followed by conjugated 12G5 (5 μg/ml) staining, referred to as cold block. CXCR4 gate was derived from cold block staining.

The number of migrated cells was measured on a Z1 Series Coulter Counter cell and particle counter (Beckman Coulter Inc.), extrapolated from the standard curve. The number of migrated PBMCs was calculated as follows: total migrated PBMCs = (the total volume of migrated cells in milliliters) × (the concentration in cells per milliliter). Input and migrated cells are phenotyped, and the percentages are obtained by flow cytometry. The number of migrated cells of each sub-population = (percentage of each subpopulation) × (total migrated PBMCs).

Blockade with CXCR4-neutralizing antibody or PTX

Freshly isolated PBMCs were incubated with CXCR4-neutralizing antibody 12G5 (0.1 μg/ml) or mouse isotype IgG2A for 15 min at 37°C immediately followed by transmigration assay. To determine the role of $G\alpha_i$ signaling, we incubated PBMCs with PTX (20 ng/ml) for 20 min and washed them, followed by transmigration assay.

Monocyte or lymphocyte isolation

Lymphocytes were isolated from PBMCs with CD14 MicroBeads and an autoMACS separator (Miltenyi Biotec) according to the manufacturer's instruction. The cells from the negative column (mainly T and B cells) were resuspended at 4×10^5 cells/ml in TEM

buffer. Monocytes were isolated from PBMCs with EasySep Human Monocyte Enrichment without CD16 Depletion kit. In monocyte repletion assays, monocytes were added back to lymphocyte suspension to a final concentration of 1×10^5 monocytes/ml and used in transmigration or adhesion assay. The purity of isolated cells was verified by flow cytometry as shown in Fig. 4, A and B.

Parallel plate flow chamber adhesion assay

THBMECs were cultured on a 35-mm tissue culture dish and activated with cytokine cocktail for 24 hours. CXCL12 (25 ng/ml) was incubated with aTHBMECs for 10 min at 37°C. Excess CXCL12 was removed by two washes, and endothelial culture was assembled into the parallel plate flow chamber as previously described (6). Monocytes and lymphocytes were isolated and labeled with CellTracker Green CMFDA and Red CMTPX, respectively, and mixed at a ratio of 1:4. PBMCs (5×10^5 cells/ml in TEM buffer) were perfused across THBMEC layer at 1 mm/s by a Medfusion 3010a syringe pump. The parallel plate flow chamber was mounted on the stage of a Leica AM Total Internal Reflection Fluorescence (TIRF) MC System (Leica Microsystems). The system was equipped with temperature controller and CO_2 incubation chamber (Leica Microsystems) to ensure that the experiments were performed at 37°C and 5% CO_2. Images were collected under a combined TIRF and epifluorescent illumination mode (TIRF-epi) with an ImageEM C9100-13 EMCCD camera (Hamamatsu), allowing for the visualization of lymphocyte-monocyte-endothelium interactions from a top-down view. Focal planes were set at the endothelial surface to visualize leukocyte-endothelial cell interactions. Video recording (20 min) of leukocyte-endothelial interaction was analyzed in NIH ImageJ software. The motions of each cell that flowed into the field and became adhesive during the shear stress application period were tracked and quantified, referred to as adhesion. The adherent cells exhibited three fates as follows: They could remain stationary throughout the period, spread and migrate over the endothelial surface without detaching, or transmigrate across the endothelial cell barriers and leave the focal plane.

CXCL12 cytochemical staining

THBMECs were cultured on coverslips and activated for 24 hours. CellTracker Green CMFDA was incubated with aTHBMECs for 30 min. Apical CXCL12 was then applied for 10 min, and excess CXCL12 was removed by two washes. Cells were incubated with CXCL12 antibody (5 μg/ml) in TEM buffer for 5 min at room temperature and immediately fixed with 4% paraformaldehyde for 15 min. Cells were further incubated in goat anti-rabbit Alexa Fluor 594 secondary antibody in phosphate-buffered saline (PBS) containing 10% goat serum for 15 min at room temperature. Cells were washed and coverslipped before being visualized on the confocal microscope. Images were analyzed with Imaris software (Bitplane Inc.).

Statistical analysis

Student's paired *t* test analyses were performed to ascertain statistical significance. A P value of <0.05 was used to establish significance.

Supplementary Material

Refer to Web version on PubMed Central for supplementary material.

Acknowledgments

We thank M. F. Stins (Johns Hopkins University) for providing THBMECs and the NIH AIDS Research and Reference Reagent Program for donating mouse anti-CXCR4 monoclonal antibody 12G5.

Funding: R.M.R. is supported by NIH grants R2174820, K2451400, and P5038667 (Project 1); support is also provided by the Williams Family Foundation for MS Research.

REFERENCES AND NOTES

1. Bartholomäus I, Kawakami N, Odoardi F, Schläger C, Miljkovic D, Ellwart JW, Klinkert WE, Flügel-Koch C, Issekutz TB, Wekerle H, Flügel A. Effector T cell interactions with meningeal vascular structures in nascent autoimmune CNS lesions. Nature. 2009; 462:94–98. [PubMed: 19829296]
2. Ransohoff RM. Immunology: In the beginning. Nature. 2009; 462:41–42. [PubMed: 19890316]
3. Engelhardt B, Ransohoff RM. The ins and outs of T-lymphocyte trafficking to the CNS: Anatomical sites and molecular mechanisms. Trends Immunol. 2005; 26:485–495. [PubMed: 16039904]
4. Ransohoff RM, Kivisäkk P, Kidd G. Three or more routes for leukocyte migration into the central nervous system. Nat Rev Immunol. 2003; 3:569–581. [PubMed: 12876559]
5. Engelhardt B. Molecular mechanisms involved in T cell migration across the blood–brain barrier. J Neural Transm. 2006; 113:477–485. [PubMed: 16550326]
6. Man S, Tucky B, Bagheri N, Li X, Kochar R, Ransohoff RM. α4 Integrin/FN-CS1 mediated leukocyte adhesion to brain microvascular endothelial cells under flow conditions. J Neuroimmunol. 2009; 210:92–99. [PubMed: 19345424]
7. Chui R, Dorovini-Zis K. Regulation of CCL2 and CCL3 expression in human brain endothelial cells by cytokines and lipopolysaccharide. J Neuroinflammation. 2010; 7:1. [PubMed: 20047691]
8. Fox RJ, Kivisäkk P, Lee JC, Tucky B, Lucchinetti C, Rudick RA, Ransohoff RM. Chemokine receptors as biomarkers in multiple sclerosis. Dis Markers. 2006; 22:227–233. [PubMed: 17124344]
9. Khatri BO, Man S, Giovannoni G, Koo AP, Lee JC, Tucky B, Lynn F, Jurgensen S, Woodworth J, Goelz S, Duda PW, Panzara MA, Ransohoff RM, Fox RJ. Effect of plasma exchange in accelerating natalizumab clearance and restoring leukocyte function. Neurology. 2009; 72:402–409. [PubMed: 19188571]
10. Ransohoff RM. Natalizumab for multiple sclerosis. N Engl J Med. 2007; 356:2622–2629. [PubMed: 17582072]
11. Charo IF, Ransohoff RM. The many roles of chemokines and chemokine receptors in inflammation. N Engl J Med. 2006; 354:610–621. [PubMed: 16467548]
12. Schreiber TH, Shinder V, Cain DW, Alon R, Sackstein R. Shear flow-dependent integration of apical and subendothelial chemokines in T-cell transmigration: Implications for locomotion and the multistep paradigm. Blood. 2007; 109:1381–1386. [PubMed: 17038526]
13. Moore CA, Milano SK, Benovic JL. Regulation of receptor trafficking by GRKs and arrestins. Annu Rev Physiol. 2007; 69:451–482. [PubMed: 17037978]
14. Borroni EM, Mantovani A, Locati M, Bonecchi R. Chemokine receptors intracellular trafficking. Pharmacol Ther. 2010; 127:1–8. [PubMed: 20451553]
15. Mahad D, Callahan MK, Williams KA, Ubogu EE, Kivisäkk P, Tucky B, Kidd G, Kingsbury GA, Chang A, Fox RJ, Mack M, Sniderman MB, Ravid R, Staugaitis SM, Stins MF, Ransohoff RM. Modulating CCR2 and CCL2 at the blood–brain barrier: Relevance for multiple sclerosis pathogenesis. Brain. 2006; 129:212–223. [PubMed: 16230319]
16. Sørensen TL, Tani M, Jensen J, Pierce V, Lucchinetti C, Folcik VA, Qin S, Rottman J, Sellebjerg F, Strieter RM, Frederiksen JL, Ransohoff RM. Expression of specific chemokines and chemokine receptors in the central nervous system of multiple sclerosis patients. J Clin Invest. 1999; 103:807–815. [PubMed: 10079101]
17. Trebst C, Ransohoff RM. Investigating chemokines and chemokine receptors in patients with multiple sclerosis: Opportunities and challenges. Arch Neurol. 2001; 58:1975–1980. [PubMed: 11735771]
18. Stumm RK, Rummel J, Junker V, Culmsee C, Pfeiffer M, Krieglstein J, Höllt V, Schulz S. A dual role for the SDF-1/CXCR4 chemokine receptor system in adult brain: Isoform-selective regulation of SDF-1 expression modulates CXCR4-dependent neuronal plasticity and cerebral leukocyte recruitment after focal ischemia. J Neurosci. 2002; 22:5865–5878. [PubMed: 12122049]

19. Rostasy K, Egles C, Chauhan A, Kneissl M, Bahrani P, Yiannoutsos C, Hunter DD, Nath A, Hedreen JC, Navia BA. SDF-1α is expressed in astrocytes and neurons in the AIDS dementia complex: An in vivo and in vitro study. J Neuropathol Exp Neurol. 2003; 62:617–626. [PubMed: 12834106]
20. McCandless EE, Piccio L, Woerner BM, Schmidt RE, Rubin JB, Cross AH, Klein RS. Pathological expression of CXCL12 at the blood-brain barrier correlates with severity of multiple sclerosis. Am J Pathol. 2008; 172:799–808. [PubMed: 18276777]
21. McCandless EE, Zhang B, Diamond MS, Klein RS. CXCR4 antagonism increases T cell trafficking in the central nervous system and improves survival from West Nile virus encephalitis. Proc Natl Acad Sci USA. 2008; 105:11270–11275. [PubMed: 18678898]
22. McCandless EE, Wang Q, Woerner BM, Harper JM, Klein RS. CXCL12 limits inflammation by localizing mononuclear infiltrates to the perivascular space during experimental autoimmune encephalomyelitis. J Immunol. 2006; 177:8053–8064. [PubMed: 17114479]
23. Burns JM, Summers BC, Wang Y, Melikian A, Berahovich R, Miao Z, Penfold ME, Sunshine MJ, Littman DR, Kuo CJ, Wei K, McMaster BE, Wright K, Howard MC, Schall TJ. A novel chemokine receptor for SDF-1 and I-TAC involved in cell survival, cell adhesion, and tumor development. J Exp Med. 2006; 203:2201–2213. [PubMed: 16940167]
24. Li M, Ransohoff RM. Multiple roles of chemokine CXCL12 in the central nervous system: A migration from immunology to neurobiology. Prog Neurobiol. 2008; 84:116–131. [PubMed: 18177992]
25. Rot A, von Andrian UH. Chemokines in innate and adaptive host defense: Basic chemokinese grammar for immune cells. Annu Rev Immunol. 2004; 22:891–928. [PubMed: 15032599]
26. Wang Y, Li G, Stanco A, Long JE, Crawford D, Potter GB, Pleasure SJ, Behrens T, Rubenstein JL. CXCR4 and CXCR7 have distinct functions in regulating interneuron migration. Neuron. 2011; 69:61–76. [PubMed: 21220099]
27. Marques CP, Kapil P, Hinton DR, Hindinger C, Nutt SL, Ransohoff RM, Phares TW, Stohlman SA, Bergmann CC. CXCR3-dependent plasma blast migration to the central nervous system during viral encephalomyelitis. J Virol. 2011; 85:6136–6147. [PubMed: 21507985]
28. Izikson L, Klein RS, Charo IF, Weiner HL, Luster AD. Resistance to experimental autoimmune encephalomyelitis in mice lacking the CC chemokine receptor (CCR2). J Exp Med. 2000; 192:1075–1080. [PubMed: 11015448]
29. Fife BT, Huffnagle GB, Kuziel WA, Karpus WJ. CC chemokine receptor 2 is critical for induction of experimental autoimmune encephalomyelitis. J Exp Med. 2000; 192:899–905. [PubMed: 10993920]
30. Huang D, Shi FD, Jung S, Pien GC, Wang J, Salazar-Mather TP, He TT, Weaver JT, Ljunggren HG, Biron CA, Littman DR, Ransohoff RM. The neuronal chemokine CX3CL1/fractalkine selectively recruits NK cells that modify experimental autoimmune encephalomyelitis within the central nervous system. FASEB J. 2006; 20:896–905. [PubMed: 16675847]
31. Man S, Ubogu EE, Williams KA, Tucky B, Callahan MK, Ransohoff RM. Human brain microvascular endothelial cells and umbilical vein endothelial cells differentially facilitate leukocyte recruitment and utilize chemokines for T cell migration. Clin Dev Immunol. 2008; 2008:384982. [PubMed: 18320011]
32. Ubogu EE, Callahan MK, Tucky BH, Ransohoff RM. CCR5 expression on monocytes and T cells: Modulation by transmigration across the blood–brain barrier in vitro. Cell Immunol. 2006; 243:19–29. [PubMed: 17257590]
33. Ubogu EE, Cossoy MB, Ransohoff RM. The expression and function of chemokines involved in CNS inflammation. Trends Pharmacol Sci. 2006; 27:48–55. [PubMed: 16310865]
34. Cinamon G, Shinder V, Alon R. Shear forces promote lymphocyte migration across vascular endothelium bearing apical chemokines. Nat Immunol. 2001; 2:515–522. [PubMed: 11376338]
35. Cinamon G, Grabovsky V, Winter E, Franitza S, Feigelson S, Shamri R, Dwir O, Alon R. Novel chemokine functions in lymphocyte migration through vascular endothelium under shear flow. J Leukoc Biol. 2001; 69:860–866. [PubMed: 11404368]

36. Cuvelier SL, Patel KD. Shear-dependent eosinophil transmigration on interleukin 4–stimulated endothelial cells: A role for endothelium-associated eotaxin-3. J Exp Med. 2001; 194:1699–1709. [PubMed: 11748272]
37. Stins MF, Gilles F, Kim KS. Selective expression of adhesion molecules on human brain microvascular endothelial cells. J Neuroimmunol. 1997; 76:81–90. [PubMed: 9184636]
38. Callahan MK, Williams KA, Kivisäkk P, Pearce D, Stins MF, Ransohoff RM. CXCR3 marks $CD4^+$ memory T lymphocytes that are competent to migrate across a human brain microvascular endothelial cell layer. J Neuroimmunol. 2004; 153:150–157. [PubMed: 15265673]
39. Slattery MJ, Liang S, Dong C. Distinct role of hydrodynamic shear in leukocyte-facilitated tumor cell extravasation. Am J Physiol Cell Physiol. 2005; 288:C831–C839. [PubMed: 15601752]
40. Hudetz AG, Fehér G, Kampine JP. Heterogeneous autoregulation of cerebrocortical capillary flow: Evidence for functional thoroughfare channels? Microvasc Res. 1996; 51:131–136. [PubMed: 8812768]
41. Berahovich RD, Zabel BA, Penfold ME, Lewén S, Wang Y, Miao Z, Gan L, Pereda J, Dias J, Slukvin II, McGrath KE, Jaen JC, Schall TJ. CXCR7 protein is not expressed on human or mouse leukocytes. J Immunol. 2010; 185:5130–5139. [PubMed: 20889540]
42. Deli MA, Abrahám CS, Kataoka Y, Niwa M. Permeability studies on in vitro blood–brain barrier models: Physiology, pathology, and pharmacology. Cell Mol Neurobiol. 2005; 25:59–127. [PubMed: 15962509]
43. Bernas MJ, Cardoso FL, Daley SK, Weinand ME, Campos AR, Ferreira AJ, Hoying JB, Witte MH, Brites D, Persidsky Y, Ramirez SH, Brito MA. Establishment of primary cultures of human brain microvascular endothelial cells to provide an in vitro cellular model of the blood-brain barrier. Nat Protoc. 2010; 5:1265–1272. [PubMed: 20595955]
44. Cucullo L, Hossain M, Rapp E, Manders T, Marchi N, Janigro D. Development of a humanized in vitro blood–brain barrier model to screen for brain penetration of anti-epileptic drugs. Epilepsia. 2007; 48:505–516. [PubMed: 17326793]
45. Jain P, Coisne C, Enzmann G, Rottapel R, Engelhardt B. $\alpha_4\beta_1$ integrin mediates the recruitment of immature dendritic cells across the blood-brain barrier during experimental autoimmune encephalomyelitis. J Immunol. 2010; 184:7196–7206. [PubMed: 20483748]
46. McCandless EE, Budde M, Lees JR, Dorsey D, Lyng E, Klein RS. IL-1R signaling within the central nervous system regulates CXCL12 expression at the blood-brain barrier and disease severity during experimental autoimmune encephalomyelitis. J Immunol. 2009; 183:613–620. [PubMed: 19535637]
47. Cruz-Orengo L, Holman DW, Dorsey D, Zhou L, Zhang P, Wright M, McCandless EE, Patel JR, Luker GD, Littman DR, Russell JH, Klein RS. CXCR7 influences leukocyte entry into the CNS parenchyma by controlling abluminal CXCL12 abundance during autoimmunity. J Exp Med. 2011; 208:327–339. [PubMed: 21300915]
48. Tanaka Y, Adams DH, Hubscher S, Hirano H, Siebenlist U, Shaw S. T-cell adhesion induced by proteoglycan-immobilized cytokine MIP-1β. Nature. 1993; 361:79–82. [PubMed: 7678446]
49. Huber AR, Kunkel SL, Todd RF III, Weiss SJ. Regulation of transendothelial neutrophil migration by endogenous interleukin-8. Science. 1991; 254:99–102. [PubMed: 1718038]
50. Gilat D, Hershkoviz R, Mekori YA, Vlodavsky I, Lider O. Regulation of adhesion of $CD4^+$ T lymphocytes to intact or heparinase-treated subendothelial extracellular matrix by diffusible or anchored RANTES and MIP-1β. J Immunol. 1994; 153:4899–4906. [PubMed: 7525718]
51. Ebnet K, Kaldjian EP, Anderson AO, Shaw S. Orchestrated information transfer underlying leukocyte endothelial interactions. Annu Rev Immunol. 1996; 14:155–177. [PubMed: 8717511]
52. Müller M, Carter SL, Hofer MJ, Manders P, Getts DR, Getts MT, Dreykluft A, Lu B, Gerard C, King NJ, Campbell IL. CXCR3 signaling reduces the severity of experimental autoimmune encephalomyelitis by controlling the parenchymal distribution of effector and regulatory T cells in the central nervous system. J Immunol. 2007; 179:2774–2786. [PubMed: 17709491]
53. Kuschert GS, Coulin F, Power CA, Proudfoot AE, Hubbard RE, Hoogewerf AJ, Wells TN. Glycosaminoglycans interact selectively with chemokines and modulate receptor binding and cellular responses. Biochemistry. 1999; 38:12959–12968. [PubMed: 10504268]

54. Maione TE, Gray GS, Hunt AJ, Sharpe RJ. Inhibition of tumor growth in mice by an analogue of platelet factor 4 that lacks affinity for heparin and retains potent angiostatic activity. Cancer Res. 1991; 51:2077–2083. [PubMed: 1706960]
55. Amara A, Lorthioir O, Valenzuela A, Magerus A, Thelen M, Montes M, Virelizier JL, Delepierre M, Baleux F, Lortat-Jacob H, Arenzana-Seisdedos F. Stromal cell-derived factor-1α associates with heparan sulfates through the first β-strand of the chemokine. J Biol Chem. 1999; 274:23916–23925. [PubMed: 10446158]
56. Luker KE, Steele JM, Mihalko LA, Ray P, Luker GD. Constitutive and chemokine-dependent internalization and recycling of CXCR7 in breast cancer cells to degrade chemokine ligands. Oncogene. 2010; 29:4599–4610. [PubMed: 20531309]
57. Luker KE, Gupta M, Steele JM, Foerster BR, Luker GD. Imaging ligand-dependent activation of CXCR7. Neoplasia. 2009; 11:1022–1035. [PubMed: 19794961]
58. Bhattacharyya BJ, Banisadr G, Jung H, Ren D, Cronshaw DG, Zou Y, Miller RJ. The chemokine stromal cell-derived factor-1 regulates GABAergic inputs to neural progenitors in the postnatal dentate gyrus. J Neurosci. 2008; 28:6720–6730. [PubMed: 18579746]
59. Klein RS, Rubin JB, Gibson HD, DeHaan EN, Alvarez-Hernandez X, Segal RA, Luster AD. SDF-1α induces chemotaxis and enhances Sonic hedgehog-induced proliferation of cerebellar granule cells. Development. 2001; 128:1971–1981. [PubMed: 11493520]
60. Ma Q, Jones D, Springer TA. The chemokine receptor CXCR4 is required for the retention of B lineage and granulocytic precursors within the bone marrow microenvironment. Immunity. 1999; 10:463–471. [PubMed: 10229189]
61. Proudfoot AE, Handel TM, Johnson Z, Lau EK, LiWang P, Clark-Lewis I, Borlat F, Wells TN, Kosco-Vilbois MH. Glycosaminoglycan binding and oligomerization are essential for the in vivo activity of certain chemokines. Proc Natl Acad Sci USA. 2003; 100:1885–1890. [PubMed: 12571364]
62. Murphy JW, Yuan H, Kong Y, Xiong Y, Lolis EJ. Heterologous quaternary structure of CXCL12 and its relationship to the CC chemokine family. Proteins. 2010; 78:1331–1337. [PubMed: 20077567]
63. Savarin C, Stohlman SA, Atkinson R, Ransohoff RM, Bergmann CC. Monocytes regulate T cell migration through the glia limitans during acute viral encephalitis. J Virol. 2010; 84:4878–4888. [PubMed: 20200240]

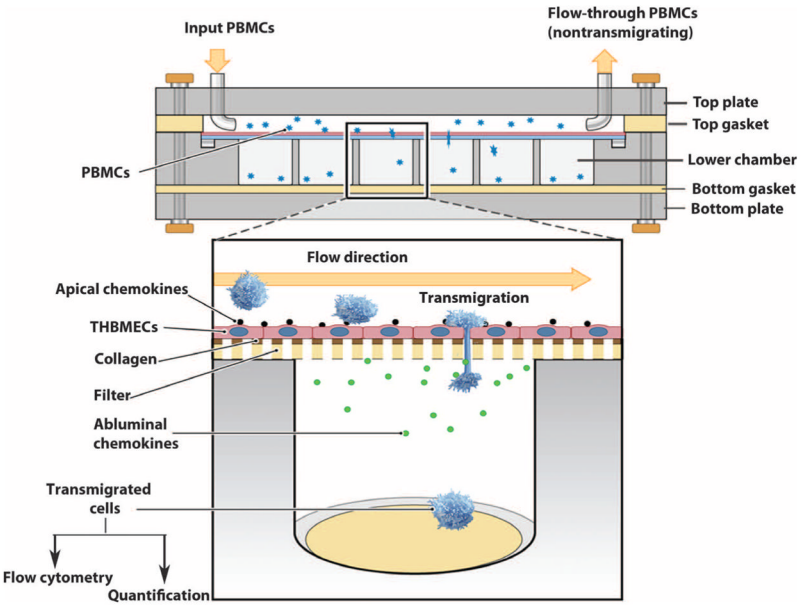

Fig. 1.

An in vitro BBB model system for studying leukocyte transmigration. This in vitro BBB model system enables flexible analysis of leukocyte migration across the BBB under physiological shear forces (flow). Shown is the flow-based chemotaxis chamber (side view) with an expanded view below. THBMECs are cultured on framed polycarbonate filters (lower image). The filter with confluent THBMECs is placed between the top and the bottom plates, and the top gasket is positioned over the filter to create a flow area. PBMCs are perfused through the inlet on the top plate across the THBMEC layer (which mimics the BBB). PBMCs that transmigrated across the THBMEC layer into the bottom chamber, together with the input PBMC population and the nontransmigrating leukocytes that passed through the system, were collected for analysis.

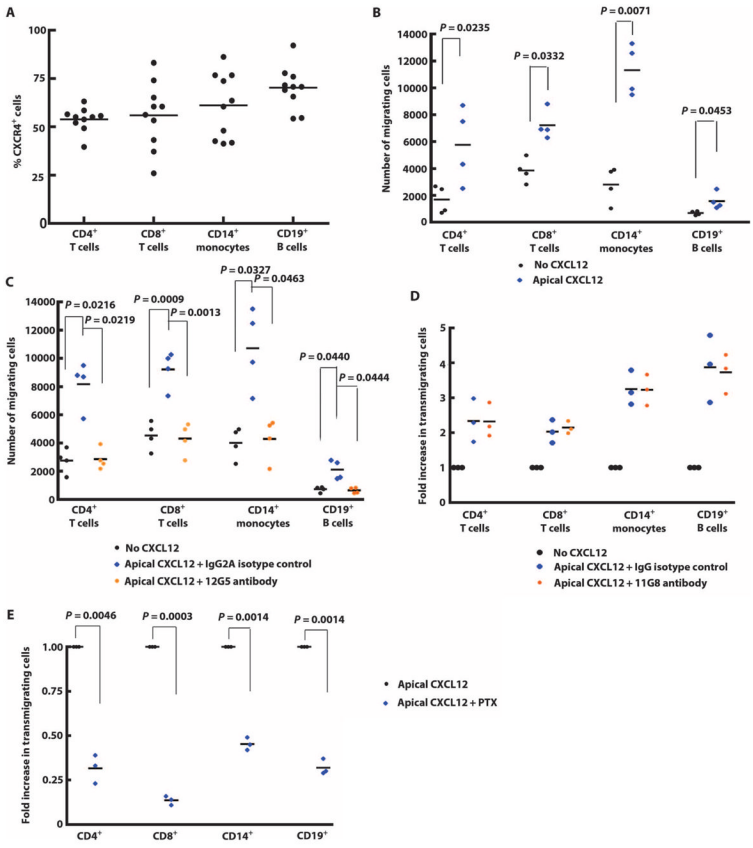

Fig. 2.

Apical CXCL12 induced PBMC transmigration. (**A**) PBMCs from human subjects were stained with fluorescence-conjugated antibodies against CD4, CD8, CD14, CD19, and CXCR4 (12G5), and analyzed by flow cytometry. Percentages of CXCR4-positive cells in each subpopulation are shown. (**B**) THBMECs were activated by incubation with IFN-γ and TNF-α, and the chemokine CXCL12 was introduced into the top chamber (apical CXCL12). The transmigration assay was performed with or without apical CXCL12, and the number of leukocytes transmigrating across THBMECs was quantified. Each symbol represents data from one experiment. (**C**) PBMCs were incubated with the CXCR4-neutralizing antibody 12G5 (0.1 μg/ml) for 15 min at 37°C immediately followed by the addition of apical CXCL12. Mouse isotype IgG2A was used as control. Each symbol represents data from one experiment. (**D**) PBMCs were incubated with CXCR7-neutralizing antibody 11G8 (0.1 μg/ml) for 20 min followed by the transmigration assay with apical CXCL12. Each symbol represents data from one experiment. (**E**) PBMCs were incubated with pertussis toxin (PTX) (20 ng/ml) for 20 min. Excess PTX was removed by two washes, and PBMCs were resuspended at 5×10^5 cells/ml in TEM buffer. Transmigration assays were performed in the presence of apical CXCL12 and absence of basolateral CCL2. Each symbol represents data from one experiment. Data were analyzed using Student's *t* test.

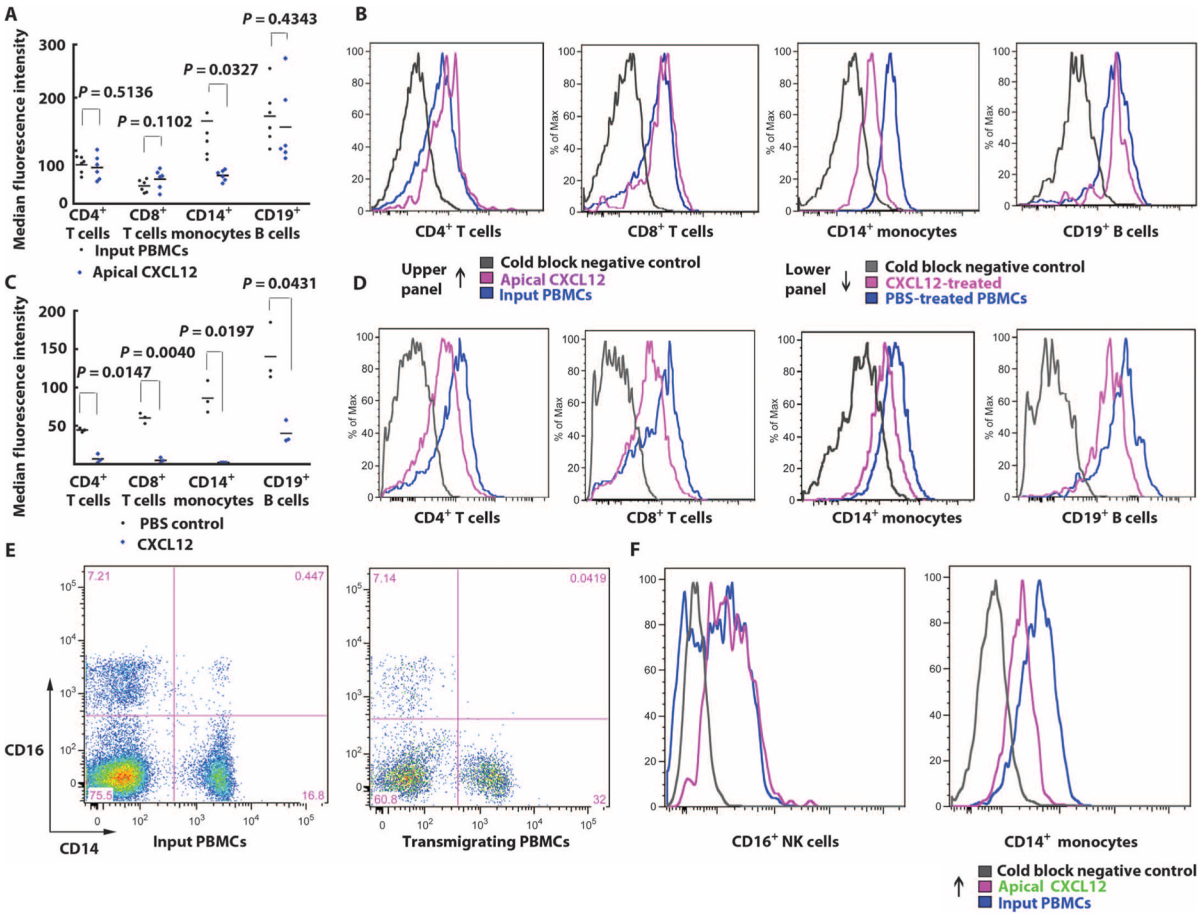

Fig. 3.

Apical CXCL12 selectively down-regulates monocyte CXCR4. (**A**) Apical CXCL12 was added to the top chamber and the transmigration assay was performed. CXCR4 expressed by transmigrating leukocytes was stained and analyzed by flow cytometry. MFI of CXCR4 expressed by each PBMC subpopulation was normalized to fluorescence beads. Each symbol represents data from one experiment. Data were analyzed using Student's *t* test. (**B**) Single-channel histogram exhibited a left shift in CXCR4 expression by transmigrating monocytes compared with the input PBMC population. Data represent six experiments. (**C**) PBMCs were incubated with CXCL12 solution (25 ng/ml) for 2 hours and then stained for CXCR4 expression and leukocyte lineage. CXCR4 MFI was normalized to fluorescence beads. Each symbol represents data from one experiment. Data were analyzed using Student's *t* test. (**D**) Single-channel histogram showing left shift in CXCR4 expression in all PBMC subpopulations. Data represent three experiments. (**E**) Monocyte subpopulations were evaluated using CD14 and CD16 as markers. In the input PBMCs (left panel), $CD14^+/CD16^-$ represented about 97% of monocytes compared with $CD14^+/CD16^+$ cells. $CD14^-/CD16^+$ cells were presumed to be NK cells. Among transmigrating cells (right panel), $CD14^+/CD16^+$ cells were not observed. (**F**) Regulation of CXCR4 expression by $CD14^+/CD16^+$ or $CD14^+/CD16^-$ or $CD14^-/CD16^+$ transmigrating cells. Single-channel histograms show that CXCR4 was not down-regulated on $CD16^+$ NK cells but was down-regulated on $CD14^+$ monocytes.

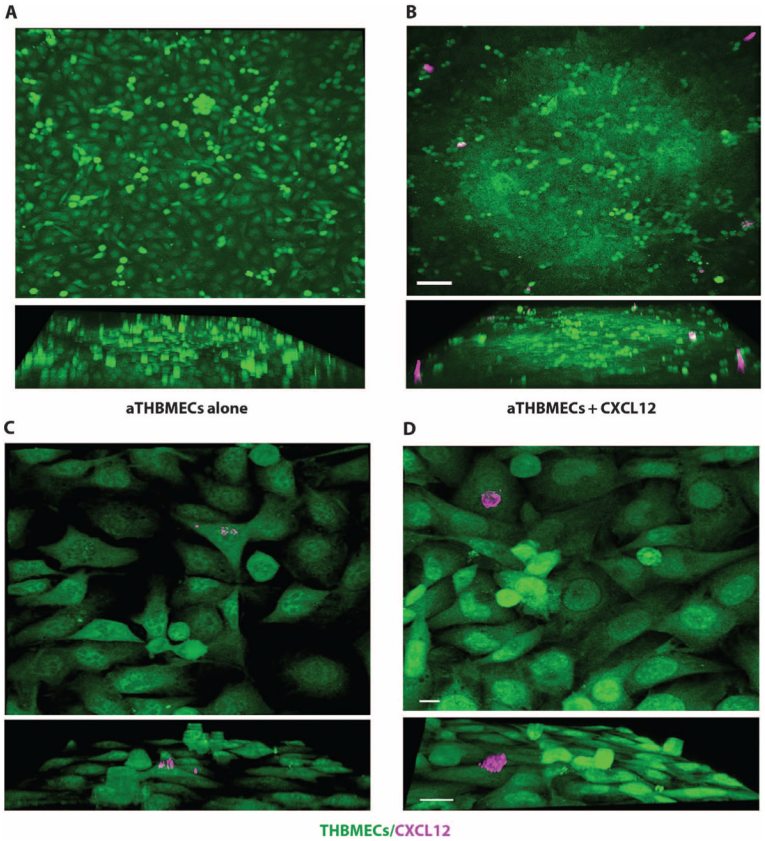

Fig. 4.

Exogenous CXCL12 accumulates on the apical surface of aTHBMECs. (**A**) THBMECs were cultured and activated on cover slides. (**B**) Apical CXCL12 was added. Live cells were stained for CXCL12. Images were collected by confocal microscopy using a 20× lens and analyzed with Imaris 3D software. Upper and side-view (lower) images show CXCL12 aggregates. aTHBMECs alone: Live-cell staining for CXCL12 was performed on aTHBMECs without exogenous CXCL12. Scale bar, 100 μm. Data represent four experiments. The color channels of images were pseudocolored to facilitate evaluation. (**C** and **D**) Images were collected using a 100× lens. Scale bars, 20 μm.

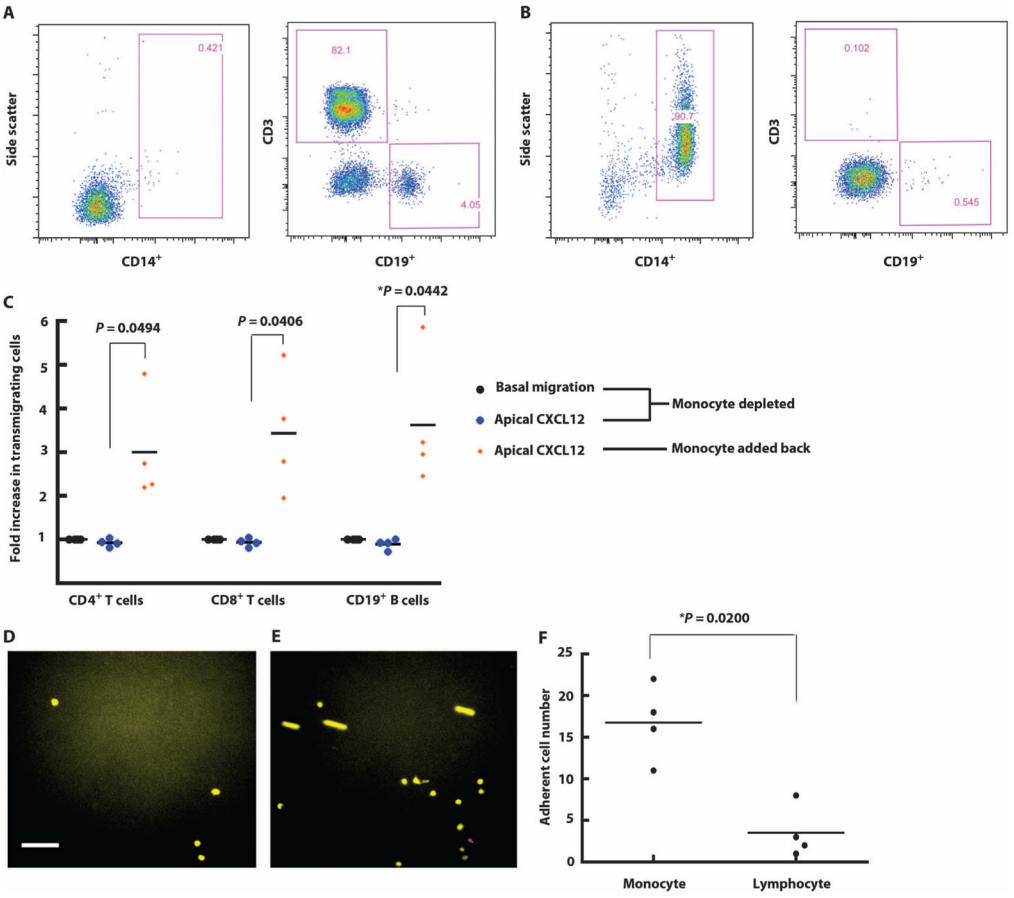

Fig. 5.

CXCL12-induced monocyte-endothelial cell interactions modulate lymphocyte transmigration. (**A**) Lymphocytes were isolated from PBMCs using negative selection. Isolated lymphocytes were stained for CD4, CD8, CD14, and CD19 markers to verify purity. (**B**) Monocytes were isolated from PBMCs using a monocyte negative selection kit. The purity was confirmed by flow cytometry. (**C**) The transmigration assay was performed in the presence or absence of apical CXCL12. Isolated lymphocytes were used as the input population at 4×10^5 lymphocytes/ml. In the group where monocytes were added back, monocytes were mixed with lymphocytes at a ratio of 1:4 as the input population with a total concentration of 5×10^5 cells/ml. The transmigration assay was performed in the presence of apical CXCL12. Each symbol represents data from one experiment. $*P < 0.05$ using Student's *t* test. (**D**) Monocytes (yellow) and lymphocytes (purple) were labeled with green and red CellTracker dye and mixed at a ratio of 1:4 as the input population. The final concentration was 5×10^5 cells/ml. The 20-min adhesion assay was performed using the parallel plate flow chamber. Images show PBMC adhesion at the beginning (D) and the end (**E**) of the assay. The color channels of images were adjusted for readers with color blindness. Scale bar, 60 μm. (**F**) Videos recording the adhesion assays were analyzed by a blinded observer on NIH ImageJ software. The motions of each cell that flowed into the field and adhered during the shear stress application period were tracked and quantified. Each symbol represents data from one experiment. $*P < 0.05$ using Student's *t* test.